CHARACTERIZATION OF FLOW-PATTERN AND HEAT TRANSFER OF MICRO FLAT HEAT PIPES

Chen-Chuan Lin[1], Kun-Lin Ho[1], Jin-Cherng Shyu[1]*, Kai-Shing Yang[2], Cheng-Wei Tu[2], Chi-Chuan Wang[3]
*Author for correspondence
[1]Department of Mechanical Engineering
National Kaohsiung University of Applied Sciences, Kaohsiung 80778, Taiwan
[2]Green Energy and Environment Research Lab.
Industrial Technology Research Institute, Hsinchu 31040, Taiwan
[3]Department of Mechanical Engineering
National Chiao Tung University, Hsinchu 30010, Taiwan
E-mail: jcshyu@kuas.edu.tw

ABSTRACT

In this study, thermal performance and flow visualization of a double layer flat micro vapor chamber are carried out. Two micro vapor chambers having pin fin and pin fin array support structure were fabricated and tested. The micro vapor chambers were composed of silicon and glass wafers having an overall size of 35 mm × 40 mm × 1.525 mm. Test results show that both the pin fin and pin fin array vapor chambers show appreciably lower thermal resistance as compared to the solid silicon counterpart, the thermal resistance of the pin fin vapor chamber is about 52-60% of the solid silicon whereas the corresponding thermal resistance of pin fin array is only 17-20 % of the solid silicon. The thermal resistance of the pin fin vapor chamber is moderately increased with the increase of supplied power whereas opposite trend is encountered for the pin fin array. The phenomenon is associated with the influence of dry-out phenomenon. It is found that the pin fin array vapor chamber is still in function even for an upside-down arrangement. The thermal resistance, however, is reduced with the rise of tilt angle, and the vertical arrangement gives the lowest thermal resistance. However, the thermal resistance is considerably increased if the heat source is placed upwards, and the corresponding thermal resistance for an upside-down heat source can be threefold higher than that of the vertical arrangement.

INTRODUCTION

In recent year, solid state lighting (e.g. LEDs) had significantly penetrated into and replaced conventional lighting market. This is associated with some of its distinguished features such as longevity, high efficiency, and environmental benign. Despite the rapid growth of LED lighting, the margin profit is also falling especially for the low power LEDs. Hence, high power LED applicable for some high-end applications had attracted a lot attention for the developers and manufacturers. Normally the high power LEDs require massive heat sink for heat dissipation, this apparently impairs the willingness of the purchase of such products from the viewpoint of the consumers for they normally expect a small volume and a low weight of the LED lighting. Currently, some manufactures had unveiled 50 W LED chip packaged in an area less than 1 cm^2 [1]. The design is capable of delivering 4300 lm brightness but also accompanied with a huge heat flux of 61.73 W/cm^2. With this enormous heat flux, a local hot spot may develop and damages the LED accordingly [2]. As a consequence, thermal management of the high power LED becomes a drastic issue that must be resolved during the design phase.

Normally, metal or ceramics are considered as the substrate of the conventional high power LED packaging. The comparatively low thermal conductivity of the substrates may jeopardize the heat dissipation path and this becomes even more pronounced when the power is raised further. Hence vapor chamber (flat heat pipe) is regarded as an effective means for high power concentrated heat sources, e.g. LED. The vapor chamber is one of the promising heat transfer devices capable of removing high heat fluxes due to its two-dimension heat spreading feature. The basic principle of operation of a vapor chamber is well understood. It uses a passive two-phase fluid to transfer heat from the evaporator to the condenser surface. The vapor chamber is a confined space with wick structure for liquid transport. The effective thermal conductivity for vapor chamber is much superior to the solid metal. There had been some studies [3, 4] employing heat pipe and heat spreader for the LED cooling. Boukhanouf et al. [5] used IR camera to compare the performance between a solid copper and a copper vapor chamber. They found that the spreading resistance is

reduced from 0.0278 °C /W (solid copper) to 0.0007 °C/W (vapor chamber) at a supplied heat flux of 28 W/cm^2. Wang et al. [6] found that the effective thermal conductivity for a vapor chamber is as high as 870 W/m-K for a vapor chamber in a heat dissipation thermal module applicable for LED cooling.

Normally, the wick structure of a typical vapor chamber normally employs the sintering process. This process may imperil the integration and packaging of LED chip. Hence an alternative solution is to employ MEMS fabrication for a micro vapor chamber based on silicon technology. The wick structure is made available through this etching process [7-9]. Through this method, integration of the LED chip and the thermal module is easier materialized, and the thermal expansion of the associated micro vapor chamber is compatible with the manufacturing process of IC industry. Accordingly, micro vapor chamber can be integrated into the LED package for local hot spot removal. However, currently the silicon based micro vapor chamber adopted a three layer deign [10-12] where the upper and lower layer encompass the micro channels and the middle layer contains supporting structure. The design is effective in practical application. However, since the performance of the micro vapor chamber strongly depends on the two-phase flow phenomenon within the vapor chamber. The foregoing designs can only give an overall performance of the vapor chamber and the detailed flow phenomenon within the micro vapor chamber is not clearly. In this regard, it is the objective of this study to examine the flow pattern alongside the micro wick structure within the micro vapor chamber for an elaborate understanding of the operation of the micro vapor chamber. The observation is made available through an integration of a double layer design which contains a base silicon heat spreader and an upper glass layer for flow observation.

EXPERIMENTAL SETUP

A schematic of the apparatus used in the experiment is shown in Fig. 1. In addition to the micro vapor chamber sample, the experimental design involved an evaporator section, a water loop, which served as a condenser, measurement devices, a data-acquisition system and an image recording system. The evaporator section was made of a copper block (35 × 7 mm), where a power supply (GW PSM-6003) supplies heat into the heater embedded in the copper block. To minimize heat loss from the heater to the environment, a Bakelite board that has a low thermal conductivity was installed beneath the copper block. For the cooling water loop, the temperature of the water flow is maintained by a low temperature thermostat, and the cooling water was circulated in a flow rate of 10 ccm by a gear pump (Cole-Parmer, EW-75211-10). The corresponding flowrate was measured by a flow meter (Cole-Parmer, 32908-45), both of a buffer and a filter were installed in the water loop to avoid particulate fouling.

In this study, two micro vapor chambers having pin fin and pin fin array support structure were fabricated and tested. The working fluids tested in this study is distilled water with filling ratios being 27% and 32% for pin fin and pin fin array support structure, respectively. Detailed geometries and dimensions of

the tested micro vapor chambers are shown in Fig. 2(a). The micro vapor chambers were composed of silicon and glass wafers having an overall size of 35 mm × 40 mm × 1.525 mm. The micro vapor chamber contains a double layer micro structure. The lower layer is consisted of 0.15-mm-deep channels with 0.3 mm width. The micro channel is designed to provide the capillary force for liquid circulating. The depth of the upper layer is 0.45 mm with two different structures for supporting and providing space for vapor flow as shown in Fig. 2(c-d).
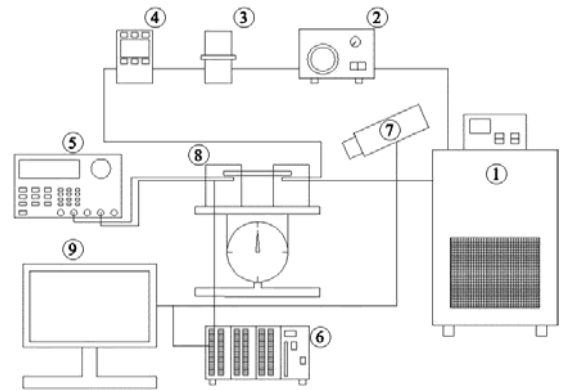
1. Thermostat; 2. Water pump; 3. Buffer and filter; 4. Flow meter; 5. Power supply; 6. Data-acquisition system; 7. High speed video camera; 8. Adjustable platform; 9. PC

(a)
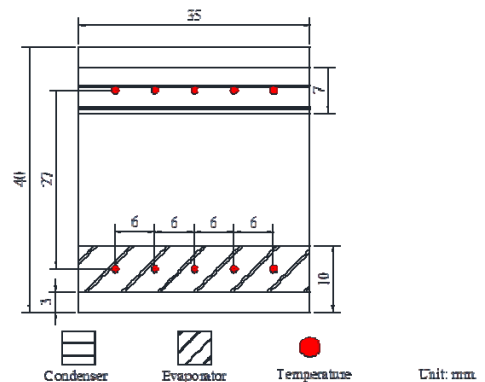
(b)

Figure 1 (a) Test facility (b) placement of the temperature measurements

The test sample was fabricated using ICP-RIE after two photolithography process as depicted in Fig. 3, and a filling hole on the glass wafer was drilled using laser machining. The SEM pictures showing both kinds of wick structure, including pin fin and pin fin array support structure, in the silicon vapor chamber were shown in Fig. 4. The silicon wafer was anodically bonded to the glass wafer. After filling the micro vapor chamber with the working fluid and sealing is imposed on the fluid filling port. For further comparison, a "Silicon-Glass" sample, which had the identical dimension as the micro

vapor chamber was made by anodic bonding of a silicon and glass wafer, was also tested in this study.

(a)

(b)

(c)

(d)
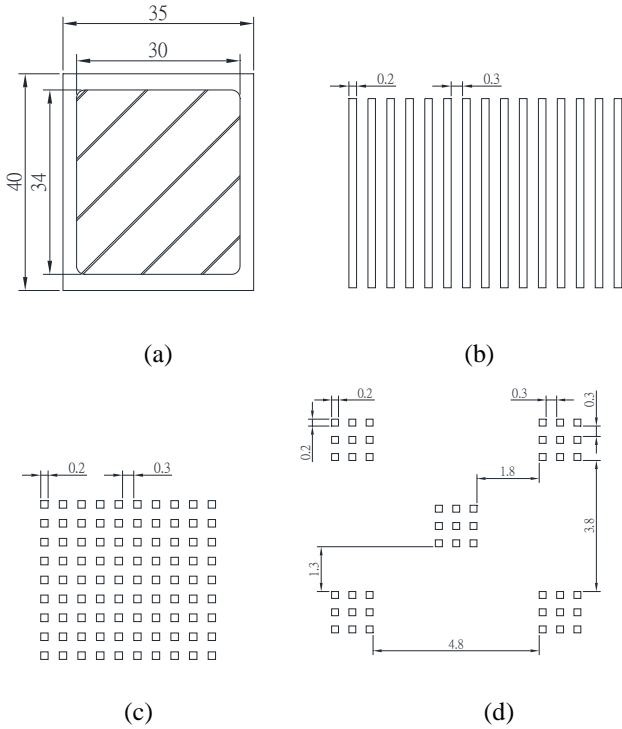
Figure 2 Micro Flat heat pipe vapor chamber (a) appearance and location of microchannel (b) microchannel at the lower layer (c) pin fin structure (d) pin fin array structure (unit: mm)

Thermocouples were used to measure the surface and fluid temperature. A total of 10 T-type thermocouples were placed underneath the test section to measure the average surface temperature, as schematically shown in Fig. 1(b), and two additional thermocouples were used to record the inlet and outlet temperatures of the cooling water in the condenser. These data signals were individually recorded and then averaged. During the isothermal test, the variation of these thermocouples was within 0.2^{0}C. In addition, all the thermocouples were pre-calibrated using a quartz thermometer that had a precision of 0.01^{0}C. The calibrated thermocouples had an accuracy of $0.1\ ^{0}$C. All the data signals were collected and converted using a data acquisition system (a hybrid recorder, Yokogawa MX-100). The data acquisition system then transmitted the converted signals through an Ethernet interface to the host computer for further operation.

Based on the measured temperature, the thermal resistance, R, is defined as follows,

$$R = \frac{T_e - T_c}{Q_a} \tag{1}$$

where T_e, T_c are the average surface temperatures in the evaporator and condenser of the heat pipe, respectively, and Q_a was estimated as the mean value of the power provided by the power supply and the heat carried away by the cooling water.

The aforementioned micro vapor chamber was located above a well-fitted Bakelite. Transparent glass was fitted on the top of the test section to enable flow visualization. Observations of the flow patterns were obtained from images recorded using a high-speed video camera (Fastec HiSpec 1.2G) and a lens that could be placed at any position above the square channel.
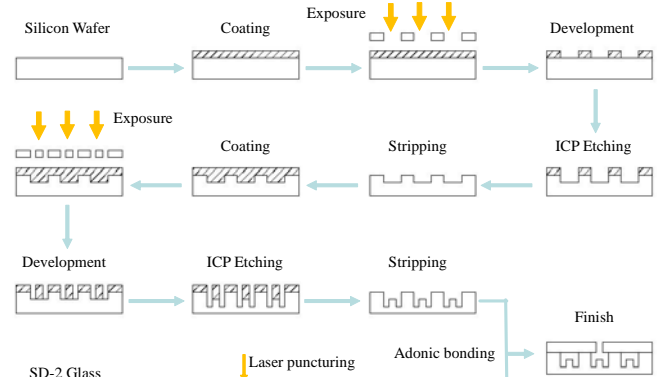
**Figure 3** Manufacturing process of the micro vapor chamber
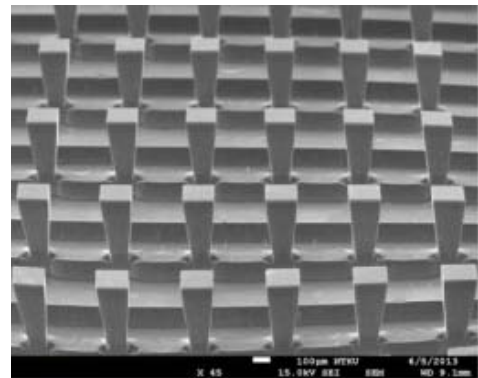
(a)
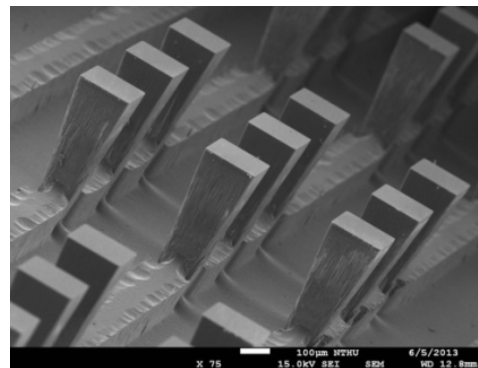
(b)

Figure 4 SEM photos of the (a) pin fin structure (b) pin fin array structure

RESULTS AND DISCUSSION

In this study, parameters affecting the performance of micro vapor chamber, including the tilt angle of the heat sources, input power, and various support of micro structure are investigated. Performance of the micro vapor chamber subject to pin fin and pin fin array structure with a vertical heat source is depicted in Fig. 5. The thermal resistance was calculated based on Eq. (1). The baseline reference is the solid silicon bonded with the glass wafer whose thermal resistance is 7.64 °C/W and it remains unchanged with the supplied power. On the other hand, the thermal resistances of the two micro vapor chambers are significantly lower than that of the solid silicon. At a supplied power of 10 W, the corresponding resistance for the pin fin and pin fin array is about 55% and 20% of the resistance of the solid silicon, implying a significant improvement of the micro vapor chambers. However, the performance of these two micro vapor chambers shows opposite trend with the supplied power. For the pin fin structure, the thermal resistance is moderately increased with the rise of supplied power. Conversely, the thermal resistance pin fin array tends to be lower with the increase of the supplied power. At a supplied power of 18 W, the thermal resistance for pin fin array is only 1.32 K/W whereas it is as high as 4.51 K/W for the pin fin structure.
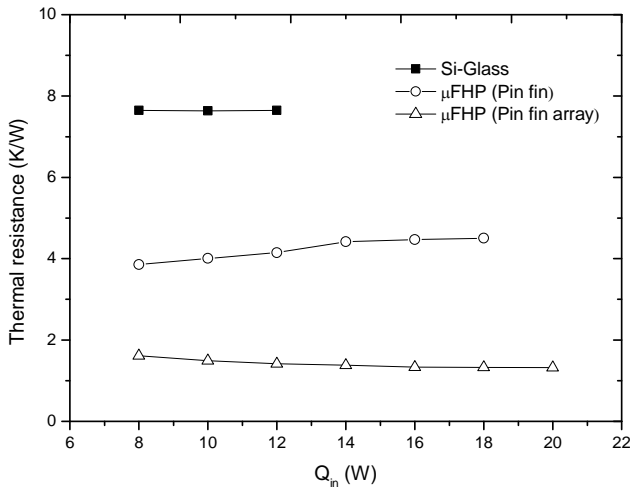
Figure 5   Thermal resistance vs. supplied power for the tested vapor chambers and solid silicon

To explain the gigantic difference, one can resort to the high speed visual recording of the flow pattern as shown in Fig. 6. Normally, the thermal resistance of heat pipes is reduced when the supplied power is increased. This is mainly associated with higher vapor flow being generated, thereby leading to a higher heat transfer performance and a lower thermal resistance. It should be noted that this is often the case when the heating surface remains comparatively wet to sustain effective evaporation. However, as clearly seen in Fig. 6 (a)-(c) applicable for the pin fin structure during the raising power process, a detectable increase of the dry-out portion prevails. This eventually gives rise to a lower heat transfer performance.

In addition, from the observed window region of Fig. 6(a)-(c), the condensate shows some aggregations alongside the microchannel, this also inhibits effective liquid/vapor circulation, and deteriorates the heat transfer performance. In summary of these two effects, a moderate increase of the thermal resistance for the pin fin vapor chamber is encountered. Conversely, as shown in Fig. 6(d)-(f), the pin fin array structure does not reveal such phenomenon where the dry out portion at the left-lower corner is about the same irrespective of the rise of supplied power. The corresponding dry-out surface relative to the total surface for the two structures vs. supplied power is shown in Fig. 6(g). Apparently the dry-out surface portion of the pin fin array is always less than 20% throughout the test range but the dry out portion for the pin fin structure exceeds 40% and approaches 50% at a supplied power of 18 W.
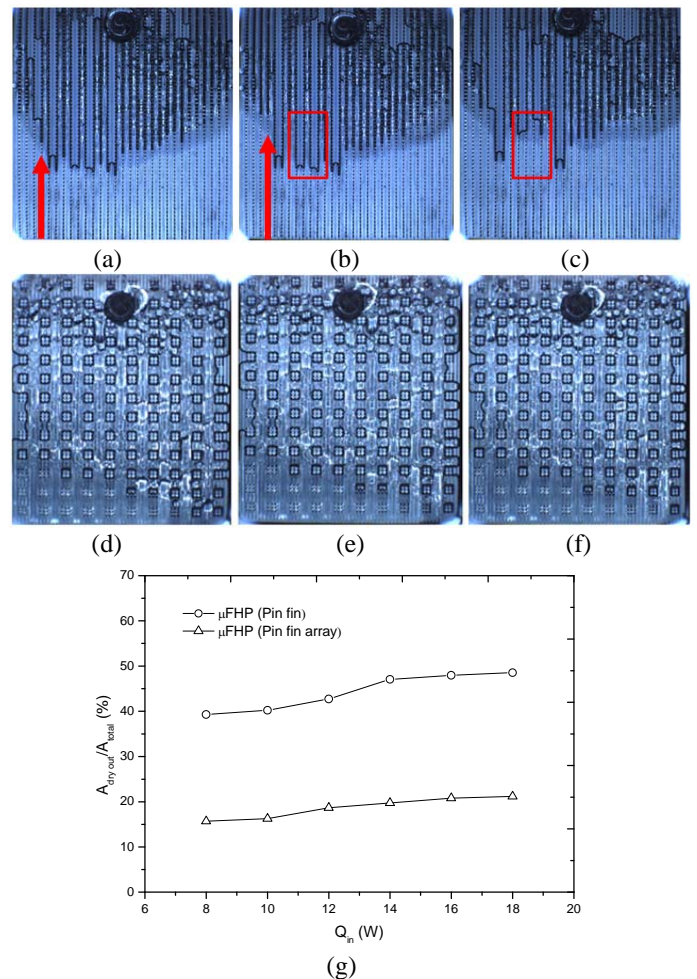

Figure 6   Observed flow pattern for the (a-c) pin fin structure (d-f) pin fin array structure; (g) dry out ratios between pin fin structure and pin fin array structure
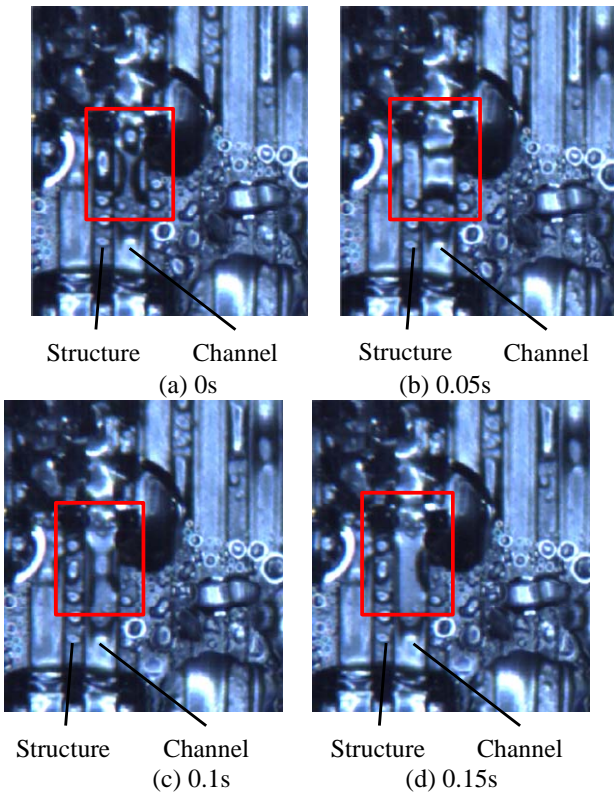
From the observation, one can realize that there are two mechanisms counteract with each other for the micro vapor chamber when the supplied power is increased. On the positive side, a higher power brings about thinner liquid layer and develops more vapor flow which may impose a better heat

transfer performance on the vapor chamber. On the down side, a higher power can also accentuate the dry out of the heating surface, yielding a lower heat transfer performance. As a result, it will result in a rise of thermal resistance if the latter mechanism offset the first one.


(a) 0s   (b) 0.05s

(c) 0.1s   (d) 0.15s
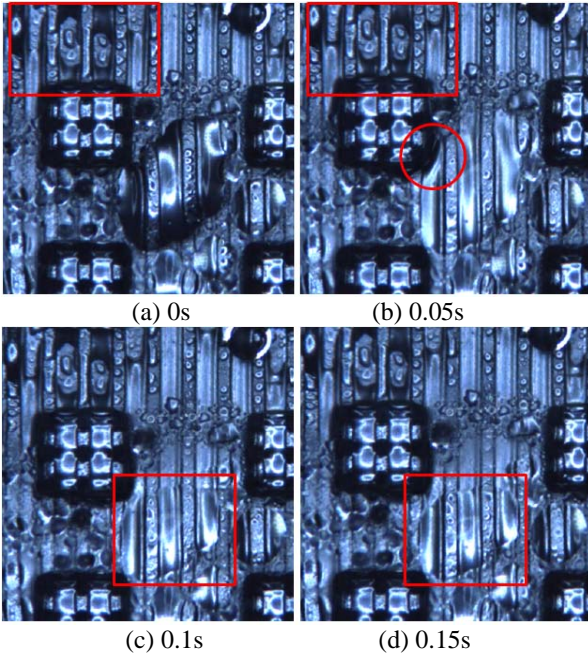
Figure 7 Condensation flow pattern of the pin fin array vapor chamber at the upper part of the condenser

Structure   Channel   Structure   Channel
(a) 0s   (b) 0.05s

Structure   Channel   Structure   Channel
(c) 0.1s   (d) 0.15s

Figure 8 Condensation flow pattern of the pin fin array vapor chamber at the channel of the condenser

For a more detailed understanding of the opposite performance of the pin fin array structure, the corresponding flow patterns at the upper part and at the channel of the condenser are schematically shown in Figs. 7 and 8. The flow pattern in the condensing portion is shown in Fig. 7(a)-(d). From the observed window outlined in the figure, one can see the condensate droplet forms on the channel as well as the glass surface, and the droplets continue to grow as time elapses. Once the growing droplet touches the wick structure, the liquid is soon drawing away by the capillary force to make room for condensation. Yet the related vapor flow generated from the evaporator is condensed on the microchannel. Hence, from the stable periodic heat removal, it would ensure a decrease of thermal resistance with supplied power.
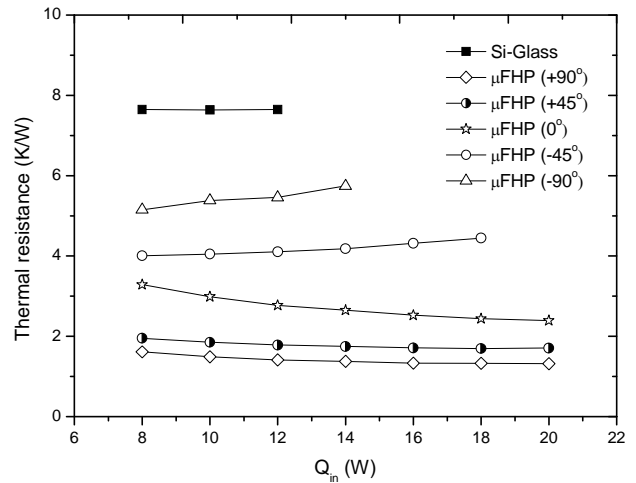
Figure 9 Effect of tilt angle on the thermal resistance subject to various supplied power for the pin fin array vapor chamber

In practical applications, although not often, the heat source may be placed in a certain tilt angle. The heat sources may be placed vertically, inclined or even upside down depending on the application. Hence, the effect of tilt angle on the performance of the pin fin array micro vapor chamber is examined and is shown in Fig. 9. Test results indicate that the vapor chamber is still in function even for an upside-down arrangement. The thermal resistance performance, however, is reduced with the rise of tilt angle, and the vertical arrangement gives the lowest thermal resistance. However, the thermal resistance is considerably increased if the heat source is placed upwards, and the corresponding thermal resistance for an upside-down heat source can be threefold higher than that of the vertical arrangement. The results are not surprising for the gravity is against the returning path of liquid condensate. The completion of liquid/vapor circulation relies on capillary force only, yet the gravity force acts against the capillary force. In addition, one can see that the thermal resistance is moderately increased with the supplied power for tilt angles of 45^0 and 90^0. The results can be made clear from the flow observation shown

in Fig. 10 where the condensate is accumulated in the bottom of vapor chamber, thereby showing a detectable rise of dry out portion. As a consequence, one can see a moderate rise of thermal resistance with the increase of supplied power.

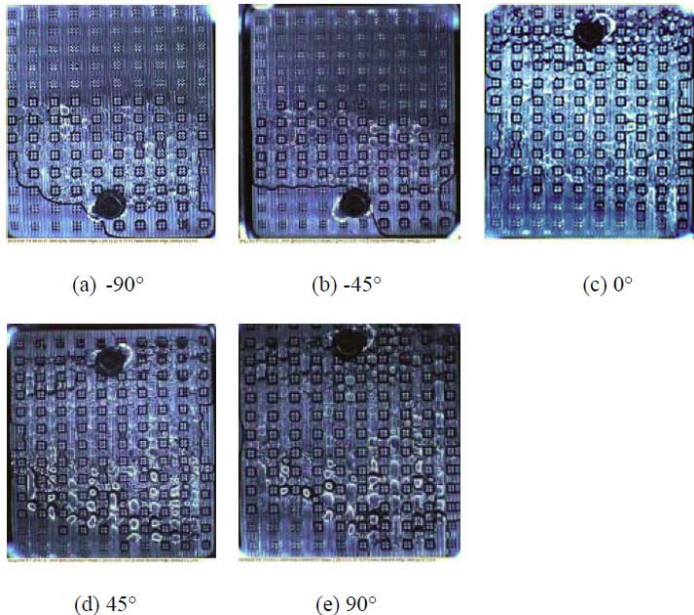(a) -90°   (b) -45°   (c) 0°

(d) 45°   (e) 90°

Figure 10   Flow observation for the pin fin array vapor chamber with different tilt angles

CONCLUSION

In this study, thermal performance and flow visualization of a double layer vapor chamber are carried out. Two micro vapor chambers having pin fin and pin fin array support structure were fabricated and tested. The working fluid tested in this study is distilled water with filling ratios being 27% and 32% for pin fin and pin fin array support structure, respectively. The micro vapor chambers were composed of silicon and glass wafers having an overall size of 35 mm × 40 mm × 1.525 mm. The micro vapor chamber contains a double layer micro structure. The effect of the tilt angle of the heat sources, input power, and support of micro structure are investigated. Based on the foregoing discussion, the following conclusions are made:

(1) Both the pin fin and pin fin array vapor chambers show appreciably lower thermal resistance as compared to the solid silicon counterpart, the thermal resistance of the pin fin vapor chamber is about 52-60% of the solid silicon whereas the corresponding thermal resistance of the pin fin array is only 17-20 % of the solid silicon.

(2) The thermal resistance of the pin fin vapor chamber is moderately increased with the increase of supplied power whereas opposite trend is encountered for the pin fin array. The phenomenon is associated with the influence of dry-out phenomenon.

(3) For the influence of tilt angle with the pin fin array vapor chamber, it is found that the vapor chamber is still in function even for an upside-down arrangement. The thermal resistance, however, is reduced with the rise of tilt angle, and the vertical arrangement gives the lowest thermal resistance. However, the thermal resistance is considerably increased if the heat source is placed upwards, and the corresponding thermal resistance for an upside down heat source can be threefold higher than that of the vertical arrangement.

REFERENCES

[1] http://www.digitimes.com.tw/tw/dt/n/shwnws.asp?cnlid=13&cat=20&id=0000313143_FPK0CNTD50PRFD2G9R2H0&ct=1, in.

[2] A. Christensen, S. Graham, Thermal effects in packaging high power light emitting diode arrays, Appl Therm Eng, 29(2-3) (2009) 364-371.

[3] L. Kim, J.H. Choi, S.H. Jang, M.W. Shin, Thermal analysis of LED array system with heat pipe, Thermochim Acta, 455(1-2) (2007) 21-25.

[4] H. Zhong, C. Zhong, W. Mingguang, Heat Dissipation for LED Lighting: Vapor Chamber Substrate Printed Circuit Board, in: Industrial Electronics and Applications (ICIEA), 2010 the 5th IEEE Conference on, 2010, pp. 565-570.

[5] R. Boukhanouf, A. Haddad, M.T. North, C. Buffone, Experimental investigation of a flat plate heat pipe performance using IR thermal imaging camera, Appl Therm Eng, 26(17-18) (2006) 2148-2156.

[6] J.C. Wang, R.T. Wang, T.L. Chang, D.S. Hwang, Development of 30 Watt high-power LEDs vapor chamber-based plate, Int J Heat Mass Tran, 53(19-20) (2010) 3990-4001.

[7] C. Gillot, Y. Avenas, N. Cezac, G. Poupon, C. Schaeffer, E. Fournier, Silicon heat pipes used as thermal spreaders, Ieee T Compon Pack T, 26(2) (2003) 332-339.

[8] S.W. Kang, S.H. Tsai, H.C. Chen, Fabrication and test of radial grooved micro heat pipes, Appl Therm Eng, 22(14) (2002) 1559-1568.

[9] S. Launay, V. Sartre, M. Lallemand, Experimental study on silicon micro-heat pipe arrays, Appl Therm Eng, 24(2-3) (2004) 233-243.

[10] Q.J. Cai, A. Bhunia, C.L. Tsai, M.W. Kendig, J.F. DeNatale, Studies of material and process compatibility in developing compact silicon vapor chambers, J Micromech Microeng, 23(6) (2013).

[11] Q.J. Cai, B.C. Chen, C.L. Tsai, Design, development and tests of high-performance silicon vapor chamber, J Micromech Microeng, 22(3) (2012).

[12] M. Ivanova, A. Lai, C. Gillot, N. Sillon, C. Schaeffer, F. Lefevre, M. Lallemand, E. Fournier, Design, fabrication and test of silicon heat pipes with radial microcapillary grooves, in: Thermal and Thermomechanical Phenomena in Electronics Systems, 2006. ITHERM '06. The Tenth Intersociety Conference on, 2006, pp. 545-551.